Available online at www.eccomasproceedia.org
Eccomas Proceedia COMPDYN (2025) 2513-2522

ECCOMAS
Proceedia

COMPDYN 2025
10th ECCOMAS Thematic Conference on
Computational Methods in Structural Dynamics and Earthquake Engineering
M. Papadrakakis, M. Fragiadakis (eds.)
Rhodes Island, Greece, 15-18 June 2025

NUMERICAL SEISMIC PERFORMANCE OF A VERNACULAR RAMMED EARTH DWELLING STRENGTHENED BY A COMPATIBLE TEXTILE REINFORCED MORTAR SYSTEM

J. D'Anna[1], D.V. Oliveira[2], R.A. Silva[2] and L. La Mendola[1]

[1] University of Palermo, Department of Engineering
Viale delle Scienze, Palermo, 90128, Italy
jennifer.danna@unipa.it; lidia.lamendola@unipa.it

[2] ISISE, University of Minho, Department of Civil Engineering
Campus de Azurém, Guimarães, 4800-058, Portugal
danvco@civil.uminho.pt; ruisilva@civil.uminho.pt

Abstract

Rammed earth buildings represent a considerable portion of the existing vernacular building stock of several countries and they are very common in the southern region of Portugal. The historical and architectural values of these constructions, along with their recognized high seismic vulnerability, have made the structural rehabilitation of earthen buildings a priority among the scientific community. Despite some recent studies, the prediction of the seismic response of these buildings is still a challenging task.

This paper presents the results of a numerical investigation on the seismic behaviour of a representative rammed earth building located in Alentejo (South of Portugal). Numerical analyses are performed on a plain and a strengthened building, by means of an advanced finite element modelling approach. A low-cost textile reinforced mortar (LC-TRM) composite is adopted to strengthen the earthen construction. Pushover analyses by mass-based lateral load pattern are performed to investigate the effect of the adopted strengthening solution. The results are discussed in terms of capacity curves and failure mechanisms.

Keywords: Rammed earth, nonlinear analysis, TRM strengthening, seismic behaviour.

ISSN:2623-3347 © 2025 The Authors. Published by Eccomas Proceedia.
Peer-review under responsibility of the organizing committee of COMPDYN 2025.
doi: 10.7712/120125.12586.26083

1 INTRODUCTION

Rammed earth constructions are made by compacting moist earth by layers inside a formwork to build monolithic walls [1][2]. The adoption of formworks constitutes a key feature, which differentiates this technique from other earth construction techniques [1][3]. Rammed earth buildings are widespread all over the world and are common in southern Portugal, where the technique was widely used not only for monuments, but also for affordable dwellings, as for instance in Alentejo, where a considerable vernacular heritage is found [4]. Moreover, during the last years, an increasing use of rammed earth has been adopted in modern constructions and this building material is attracting scientific interest because of its sustainable properties [5][6].

Recently, the structural rehabilitation of existing rammed earth buildings has drawn increasing attention due to the large number of existing earthen constructions, as well as due to their historical, architectural and cultural value. Rammed earth buildings suitably resist gravity loads, although they are considerably vulnerable to earthquakes [7][8]. Rammed earth structures are often located in high seismic hazard regions and their possible collapse could result in a significant loss of human lives, besides large economic, cultural and heritage losses. This indicates the necessity to improve the seismic performance of these structures by considering appropriate strengthening solutions.

Numerous intervention solutions are proposed in the literature in order to mitigate the vulnerability of earthen constructions, such as strengthening with boundary wooden elements [9] or ring beams [10], or the repair of cracks with grout injections [11]. The intervention on rammed earth structures requires the use of a strengthening technique able to improve its ductility, without renouncing to the requirement of compatibility with the substrate and sustainability. In this sense, textile reinforced mortars (TRM) composites have been investigated as a solution to strengthen earthen constructions against seismic actions, due to their efficiency in the strengthening of masonry buildings [11] .

Research on TRM strengthening of rammed earth started recently and the first experimental results show an improvement of the overall seismic behaviour [13][14][15]. However, available outcomes constitute a first effort and additional studies are still required to understand the role of TRM reinforcement in the structural response of rammed earth. Besides experimental studies, the response of rammed earth walls has been studied in the literature by finite element modelling (FEM) analysis, usually adopting the macro-modelling approach [16][17][18].

This work investigates the seismic performance of a vernacular rammed earth dwelling located in the south of Portugal. Numerical analyses are carried out on a plain and TRM-strengthened model, using an advanced finite element model. A compatible and low-cost textile reinforced mortar (LC-TRM) composite is chosen as reinforcement material. Pushover analyses by mass-proportional loads are performed to investigate the effect of the TRM solution. The outcomes are presented and discussed in terms of capacity curves and failure mechanisms.

2 VERNACULAR RAMMED EARTH DWELLING FROM PORTUGAL

Rammed earth constructions from the south of Portugal present typically a plan rectangular shape and a single storey. The façades are characterized by few small size openings and the main façade includes one or two doors, while openings commonly present timber lintels. The thickness of the walls is usually of 0.50 m. Most frequently, rammed earth buildings show lightweight timber shed or gable roofs, with beams supported directly on the walls. Due to the low in-plane stiffness of the roof system, rammed earth constructions do not present a box-behaviour. A typical vernacular rammed earth dwelling is depicted in Figure 1a.

3 CASE STUDY AND NUMERICAL MODEL

3.1 Building Geometry

The geometrical characteristics of the model are presented in Figure 1b. The plan dimensions of the building are equal to 8x12 m^2 and the walls have thickness of 0.5 m, with a 0.4 m high stone masonry plinth. The openings show symmetrical configuration along the X direction and are characterized by the presence of timber lintels. A gable roof with slope between 15-20 degrees was considered.

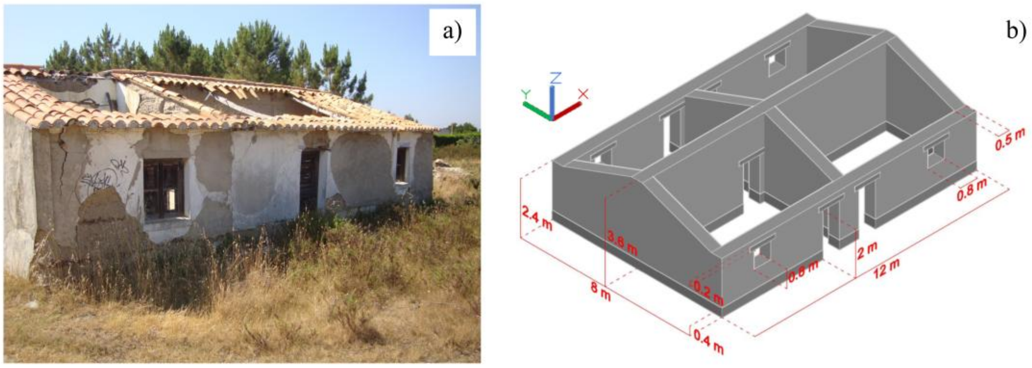

Figure 1: Rammed earth building: a) typical rammed earth dwelling from Portugal; b) geometry of the model

3.2 Finite Element Model

The modelling and analysis of the building were made by using the software DIANA 10.3 [19]. Regarding the materials, the rammed earth behaviour was simulated adopting the total strain crack model (TSRCM), using a multi-linear relationship in compression, according to previous studies [16][20], and an exponential softening model in tension, considering parameters with basis on previous numerical works [16][21]. The TSRCM was also used to simulate the material response of the stone masonry of the base plinth. In particular, a parabolic relationship was adopted to model the compressive behaviour, while the tensile response was simulated using an exponential softening model, using parameters borrowed from available numerical studies [10]. An elastic behaviour was assumed for the timber lintels, considering parameters suggested in [22]. The TRM system used in the current study was selected based on a previous experimental work [23][24] evaluating the features of different low-cost textile reinforced mortar (LC-TRM) solutions. In particular, the TRM system involved a glass fibre mesh and an earth-based mortar. The modelling of the LC-TRM material followed the approach proposed in [16], which considers the use of the TRSCM, with a tensile response characterized by a typical trilinear law obtained experimentally [23]. The compressive behaviour of the LC-TRM system is mostly dependent from the mortar and was defined considering a multi-linear experimental relationship [23]. Table 1 summarizes the material properties adopted in this study.

The nonlinear response of the plain and TRM-strengthened model was simulated by using a three-dimensional model, following a macro-modelling strategy. The rammed earth walls, the stone masonry plinth and the timber lintels were modelled as a continuum material with 20-node iso-parametric brick elements (CHX60). The roof load was applied to the longitudinal walls by using point-mass elements. The TRM system was modelled as a continuum material with 3D 8-node quadrilateral curved shell elements (CQ40S). The TRM was connected to the rammed earth by means of 16-node quadrilateral interface elements (CQ48I). Due to the absence of experimental data regarding the bond behaviour of the adopted TRM composite, a rigid connection was assumed. As for the boundary conditions, the building was assumed to be totally fixed at the base.

Material	E [MPa]	ν [-]	ρ [Kg/m^3]	f_c [MPa]	f_t [MPa]	G_f^I [N/mm]	ε_{ut} [-]
Rammed earth	1034	0.27	2000	1.28	0.05	0.074	-
Stone masonry	1500	0.20	2000	3.00	0.15	0.05	-
Timber	10000	0.20	600	-	-	-	-
LC-TRM	3431	0.27	1810	1.30	1.62	-	0.0137

E is Young's modulus, ν is Poisson's ratio, ρ is bulk density, f_c is compressive strength, f_t is tensile strength, G_f^I is mode-I tensile fracture energy and ε_{ut} is ultimate tensile strain.

Table 1: Mechanical properties of materials

4 RESULT AND DISCUSSION

The pushover analyses were performed for the +X and -X directions, see Figure 1b. In the Y direction, the model was only pushed for +Y because of its symmetry with respect to the X direction.

4.1 Plain Model

Figure 2a, b and c show the pushover curves of the plain model, in terms of seismic coefficient and lateral displacement of a control node, for +X, -X and Y directions respectively. The outcomes of +X and -X directions are comparable in terms of load and displacement capacity. The values of the maximum seismic coefficient are 0.81 and 0.82 respectively, corresponding to the same value of displacement (2 mm). Moreover, damage initiation occurs at the same value of the seismic coefficient (0.09) for both directions. The two curves show a sudden drop after the ascending branch, followed by a quite smooth capacity decrease, connected to the overturning of the external transversal wall.

The contour maps of lateral displacements and principal tensile strains at the peak capacity of the plain model pushed along +X are depicted in Fig. 3. The lateral displacements (Figure 3a) suggest that the external transversal wall pushed outside experienced the highest displacement because of the expected lower efficiency in tension of the elements counteracting the overturning movement. The highest strain values concentrate along the height of the connection between longitudinal walls and overturning wall (Figure 3b), involving the top portion of the spine wall, which evidences the tendency of the transversal wall to detach from the supporting walls and the ability of the spine wall to collaborate to the out-of-plane movement. It is noted that the compressive strength of the rammed earth is not reached at any point. The contour maps related to the -X direction are similar and are not presented here for the sake of brevity.

The pushover curve of the plain model pushed along Y direction (Fig. 2c) shows a maximum load factor of 0.62, corresponding to a displacement of 2.5 mm, higher than the peak displacement achieved along +X and -X directions (2 mm). The lower load can be explained by a less effective supporting contribution of the transversal walls in this direction, due to the geometry of the building and the presence of openings, which make this part of the structure particularly vulnerable to out-of-plane seismic forces. The damage onset occurs at a value of seismic coefficient equal to 0.05. Thus, the results point out that this is the direction which limits the performance of the plain building in terms of load capacity. The post-peak is characterized by a smooth degradation of the load capacity.

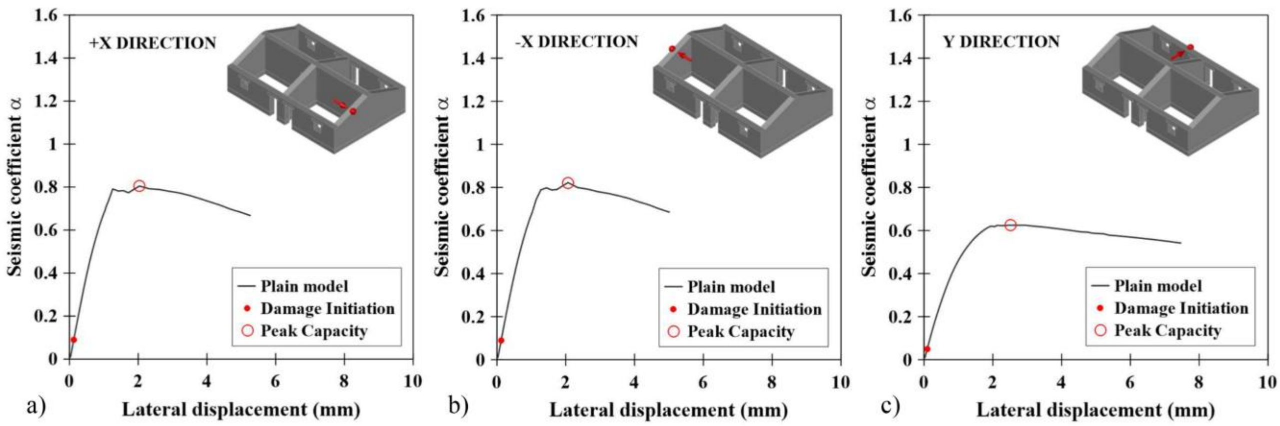

Figure 2: Pushover curves of the plain model pushed in a) +X direction, b) -X direction, c) Y direction

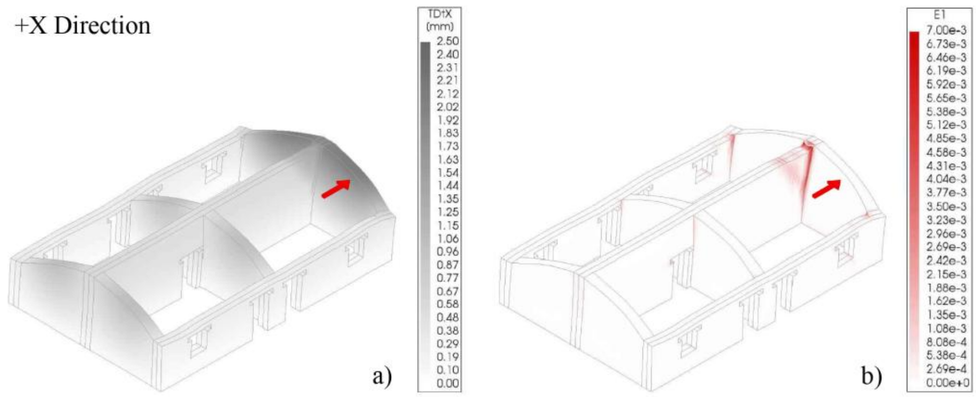

Figure 3: Plain model pushed in +X direction: a) total lateral displacements and b) principal tensile strains at peak capacity

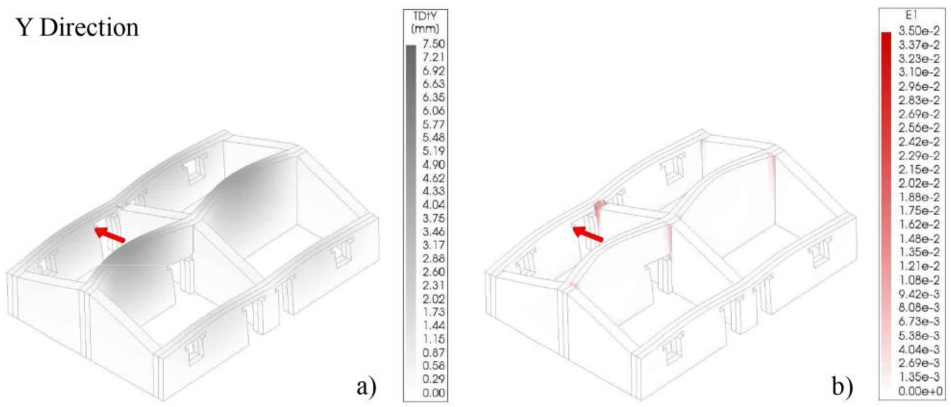

Figure 4: Plain model pushed in Y direction: a) total lateral displacements and b) principal tensile strains at peak capacity

The contour maps at the peak capacity of the model pushed along Y direction are presented in Figure 4. The highest values of lateral displacement are located at the middle spans of the spine wall (Figure 4a), even if considerable high values are also observed in the external longitudinal wall. The principal tensile strains indicate that the main failure mechanism is associated to the out-of-plane movement of the external longitudinal wall, as evidenced by the high strain values at the intersection between overturning wall and central transversal wall (Figure 4b).

4.2 TRM-Strengthened Model

The pushover curves of the TRM-strengthened model are presented in Figure 5a, b and c for +X, -X and Y directions, respectively. The pushover curves of the plain model are also reported for comparison. Considering +X and -X directions, the TRM system slightly increases the pre-peak stiffness of the model and it does not considerably modify the onset of damage, which tends to initiate in the rammed earth. On the other hand, the strengthening system increases the load capacity and the corresponding lateral displacement by 13% and 132 % respectively, in the case of +X direction, with respect to the plain model, and by 9% and 144% for -X direction.

The contours of principal tensile strains in rammed earth for both plain and strengthened model pushed along +X direction are depicted in Figure 6a, b and c, along with the individual strain contour of the LC-TRM strengthening system (Figure 6d). The strengthened model at the peak capacity of the plain model (Figure 6b) shows a reduction of the tensile strain values at the intersection between longitudinal walls and external transversal wall, proving an increased integrity of the wall thanks to the application of the TRM system, which allows to redistribute the stresses and limit the tendency to overturn. Figure 6c shows that the failure mechanism of the strengthened model is similar to that of the plain model, but the highest strain values are not concentrated at the intersection between spine and external transversal wall, but are distributed over a larger portion of the spine wall, which indicates that a higher lateral load is needed to initiate the collapse of the structure. As for the damage in the TRM elements, Figure 6d points out a contribution of the TRM to the stress transferring in areas of the rammed earth prone to fail (base of the rammed earth structure connected to the plinth, connection between longitudinal walls and transversal overturning wall, and close portion of the spine wall involved in the failure mechanism). Thus, the TRM system effectively contributes to improve the out-of-plane response of the model. The contour plots of the model pushed in -X direction are not presented for the sake of brevity; however, it is worth noting that the failure mechanism activated is the same as that along +X direction.

The pushover curve of the strengthened model pushed along the Y direction (Figure 5c) shows that, even in this case, the application of the TRM slightly increases the pre-peak stiffness, but has no important influence on the damage onset. The strengthening system guaranteed a load capacity gain of 31%, higher than that achieved for +X and -X direction, while the increase of the corresponding displacement (68%) was lower than that in the other directions.

The contours of the principal tensile strains in rammed earth for the plain and strengthened model pushed in the Y direction are reported in Figure 7a, b and c. The strengthened model at the peak capacity of the plain model (Figure 7b) highlights a noticeable reduction of the values of principal tensile strains, which means that the detachment of the external longitudinal wall from the central transversal wall is delayed. Indeed, the TRM system improves the integrity and lateral stiffness of the longitudinal walls, which become able to redistribute the stresses and show lower tendency to overturn. The contour of principal tensile strains of the strengthened model at its peak capacity (Figure 7c) shows that the final collapse mechanism is similar to that of the plain model. Higher strain values interest larger portions of the intersection between the transversal walls and the external longitudinal wall, suggesting that a higher lateral load is required to initiate the failure mechanism. Considering the damage of the LC-

TRM system at the peak capacity of the strengthened model (Figure 7d), it is evident that the composite contributes to the stress transfer in the zones of rammed earth that endure higher stresses.

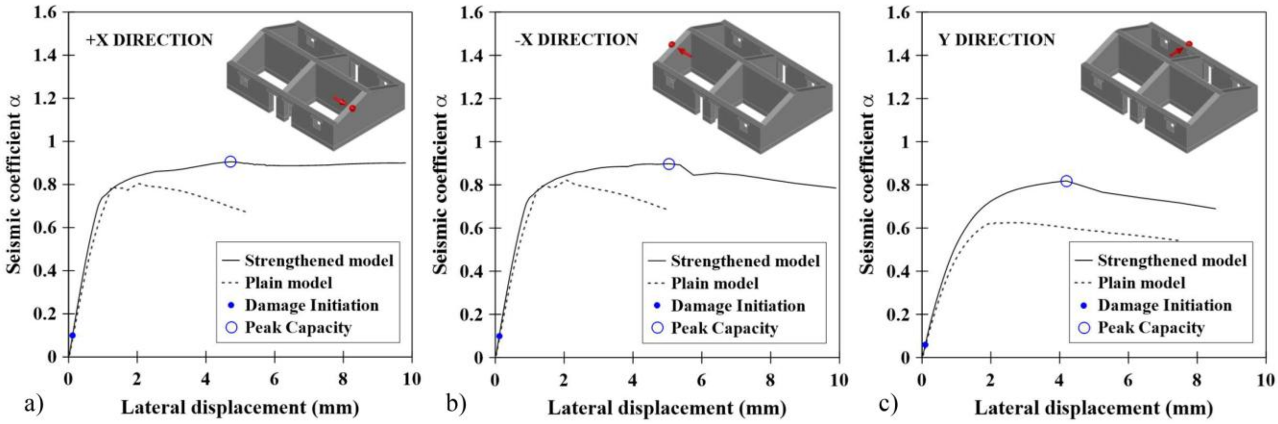

Figure 5: Pushover curves of the TRM-strengthened model pushed in a) +X direction, b) -X direction, c) Y direction

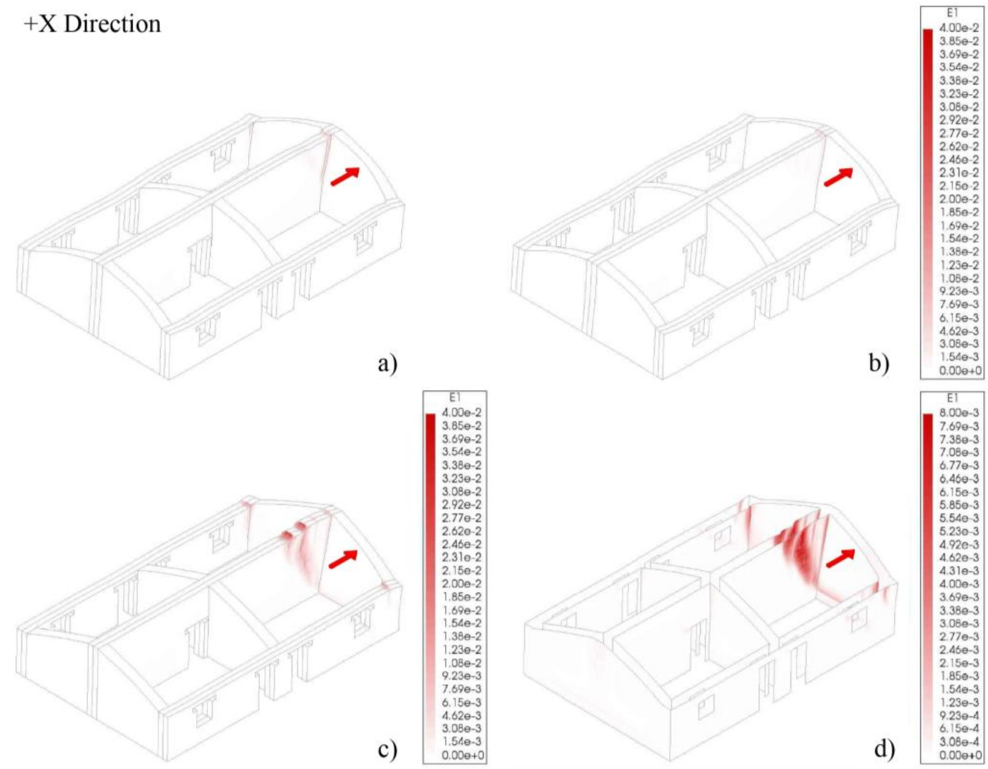

Figure 6: Principal tensile strains of the TRM-strengthened model pushed in +X direction: a) plain model at its peak capacity, b) strengthened model at the peak capacity of the plain model, c) strengthened model at its peak capacity; d) LC-TRM at the peak capacity of the strengthened model

5 CONCLUSIONS

This paper presents a numerical study on the seismic performance of a representative rammed earth dwelling typical from the south of Portugal and investigates the effect of a low-cost TRM strengthening system, by performing a series of pushover analyses.

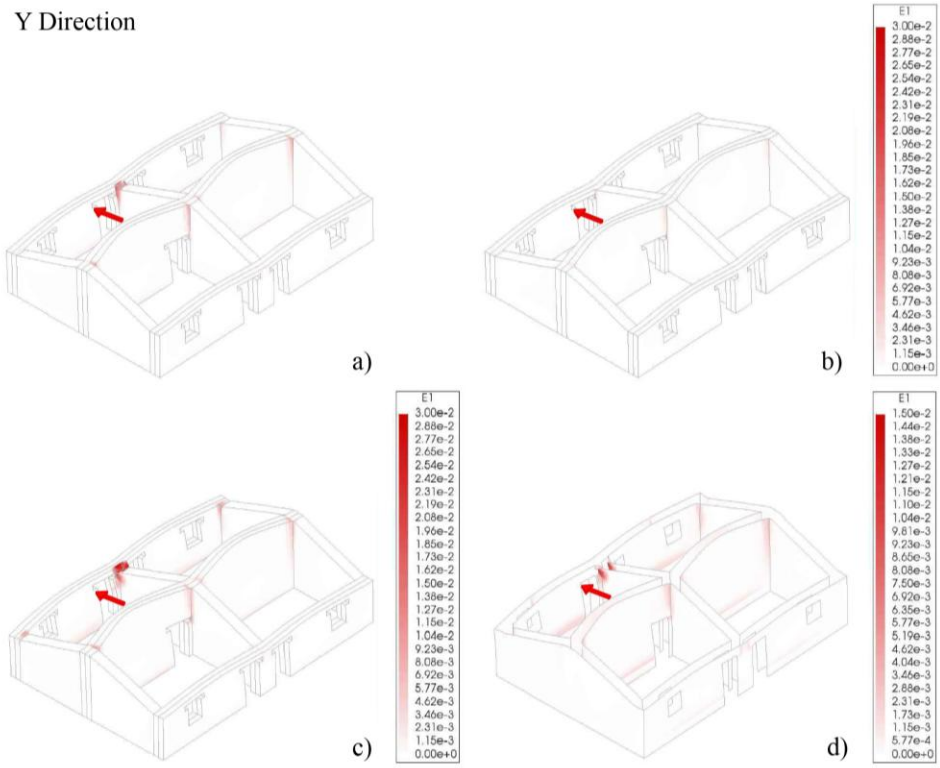

Figure 7: Principal tensile strains of the TRM-strengthened model pushed in Y direction: a) plain model at its peak capacity, b) strengthened model at the peak capacity of the plain model, c) strengthened model at its peak capacity; d) LC-TRM at the peak capacity of the strengthened model

It was observed that the failure mechanism of the plain model was controlled by the detachment and overturning of the external transversal wall for X direction, and the external longitudinal wall for Y direction. The critical direction, limiting the performance of plain model in terms of load capacity, is the Y direction, with a maximum load factor of 0.62; higher values (0.81 and 0.82) were reached for the X direction. The damage onset occurred always at very low values of lateral load because of the marked nonlinear response of rammed earth.

The LC-TRM strengthening system slightly increased the pre-peak lateral stiffness of the model, but did not promote a delay of the damage initiation. On the other hand, improvements were observed for the load capacity and for the ultimate displacement mainly, with gains of 13% and 132% for +X direction, and increments of 9% and 144% for -X direction, respectively. The load increase was much higher and equal to 31% for Y direction, while the corresponding displacement gain was of 68%, then lower than that in the other directions.

REFERENCES

[1] H. Houben, H. Guillaud. Earth construction – a comprehensive guide. 3rd ed. London, UK: CRATerre – EAG, Intermediate Technology Publication; (2008).

[2] H. Schroeder. Sustainable building with earth. Switzerland: Springer International Publishing; (2016).

[3] G. Minke. Earth construction handbook, WIT press, Boston; (2003).

[4] M. Correia. Rammed earth in Alentejo. Lisbon: Argumentum; (2007).

[5] L. Soudani, A. Fabbri, J.C. Morel, M. Woloszyn, P.A. Chabriac, H. Wong, et al. Assessment of the validity of some common assumptions in hygrothermal modeling of earth based materials. Energy and Buildings 116 (2016): 498-511.

[6] B. Bolborea, C. Baeră, A. Gruin, A. C. Vasile, and A. M. Barbu. A review of non-destructive testing methods for structural health monitoring of earthen constructions. Alexandria Engineering Journal 114 (2025): 55-81.

[7] Romanazzi, D. V. Oliveira, R. A. Silva, P. X. Candeias, A. Campos Costa, and A. Carvalho. Out-of-plane shake table test of a rammed earth sub-assembly. Bulletin of Earthquake Engineering 20, no. 15 (2022): 8325-8356.

[8] Romanazzi, D. V. Oliveira, R. A. Silva, A. Barontini and N. Mendes. Performance of rammed earth subjected to in-plane cyclic displacement. Materials and structures 55, no. 2 (2022): 54.

[9] L.E. Yamin, C.A. Philips, J.C. Reyes, D.M. Ruiz. Seismic behavior and rehabilitation alternatives for adobe and rammed earth buildings. In Proceedings of the 13th world conference on earthquake engineering, Vancouver, BC, Canada, pp. 1-6. (2004).

[10] C. Librici. Modeling of the Seismic Performance of a Rammed Earth Building. Master Thesis. Portugal: University of Minho, Guimarães; (2016).

[11] R. A. Silva. Repair of Earth Constructions by Means of Grout Injection. PhD Thesis. Portugal: University of Minho, Guimarães; (2013).

[12] G. De Felice, S. De Santis, L. Garmendia, B. Ghiassi, P. Larrinaga, P.B. Lourenço, et al. Mortar-based systems for externally bonded strengthening of masonry." Materials and structures 47 (2014): 2021-2037.

[13] K. Liu, M. Wang, and Y. Wang. 2015. Seismic retrofitting of rural rammed earth buildings using externally bonded fibers. Construction and Building Materials 100 (2015): 91-101.

[14] Y. Wang, M. Wang, K. Liu, W. Pan and X. Yang. Shaking table tests on seismic retrofitting of rammed-earth structures. Bulletin of Earthquake Engineering 15 (2017): 1037-1055.

[15] Romanazzi, D. V. Oliveira, R. A. Silva, and A. Barontini. Effectiveness of a TRM solution for rammed earth under in-plane cyclic loads. Construction and Building Materials 407 (2023): 133551.

[16] R. Barros, H. Rodrigues, H. Varum, A. Costa, and M. Correia. Seismic analysis of a Portuguese vernacular building. Journal of Architectural Engineering 24, no. 1 (2018): 05017010.

[17] R. Allahvirdizadeh, D.V. Oliveira and R.A. Silva. Numerical modeling of the seismic out-of-plane response of a plain and TRM-strengthened rammed earth subassembly. Engineering Structures, (2019), 193, 43-56.

[18] R. Allahvirdizadeh, D.V. Oliveira and R.A. Silva. Numerical investigation of the in-plane seismic performance of unstrengthened and TRM-strengthened rammed earth walls. International Journal of Architectural Heritage 15, no. 4 (2021): 548-566.

[19] DIANA, FEA. DIANA FEM-software release 10.3. (2019).

[20] L. Miccoli, D.V. Oliveira, R.A. Silva, U. Müller, L. Schueremans. "Static behaviour of rammed earth: experimental testing and finite element modelling." Materials and Structures 48 (2015): 3443-3456.

[21] R.A. Silva, D.V. Oliveira, L. Schueremans, P.B. Lourenco, T. Miranda. Modelling the structural behaviour of rammed earth components. In: Topping BHV, Iványi P, editors. Proceedings of the 12th International Conference on Computational Structures Technology. Scotland: Civil-Comp Press; (2014).

[22] J. Ortega, G. Vasconcelos, M. Correia, H. Rodrigues, P.B. Lourenço, H. Varum. (2015) Evaluation of seismic vulnerability assessment parameters for portuguese vernacular constructions with nonlinear numerical analysis. In: 5th ECCOMAS Thematic Conference on Computational Methods in Structural Dynamics and Earthquake Engineering (COMPDYN 2015).

[23] C.A. Barroso. Innovative Seismic Strengthening of Rammed Earth Constructions. MSc Thesis. Portugal: University of Minho, Guimarães; (2017) [in Portuguese].

[24] D.V. Oliveira, R.A. Silva, C. Barroso, P.B. Lourenco. Characterization of a compatible low cost strengthening solution based on the TRM technique for rammed earth. Key Engineering Materials 747 (2017): 150-157.